Dynamic cycling of eIF2 through a large eIF2B-containing cytoplasmic body

CAMPBELL, Susan <http://orcid.org/0000-0002-6740-1445>, HOYLE, Nathaniel P. and ASHE, Mark P.

Dynamic cycling of eIF2 through a large eIF2B-containing cytoplasmic body: implications for translation control

Susan G. Campbell, Nathaniel P. Hoyle, and Mark P. Ashe

Faculty of Life Science, The University of Manchester, Manchester, M13 9PT, England, UK

The eukaryotic translation initiation factor 2B (eIF2B) provides a fundamental controlled point in the pathway of protein synthesis. eIF2B is the heteropentameric guanine nucleotide exchange factor that converts eIF2, from an inactive guanosine diphosphate–bound complex to eIF2-guanosine triphosphate. This reaction is controlled in response to a variety of cellular stresses to allow the rapid reprogramming of cellular gene expression. Here we demonstrate that in contrast to other translation initiation factors, eIF2B and eIF2 colocalize to a specific cytoplasmic locus. The dynamic nature of this locus is revealed through fluorescence recovery after photobleaching analysis. Indeed eIF2 shuttles into these foci whereas eIF2B remains largely resident. Three different strategies to decrease the guanine nucleotide exchange function of eIF2B all inhibit eIF2 shuttling into the foci. These results implicate a defined cytoplasmic center of eIF2B in the exchange of guanine nucleotides on the eIF2 translation initiation factor. A focused core of eIF2B guanine nucleotide exchange might allow either greater activity or control of this elementary conserved step in the translation pathway.

Introduction

The initiation of eukaryotic protein synthesis is a highly regulated step in the gene expression pathway. One of the fundamental controlled points in translation initiation involves the recycling of eukaryotic initiation factor 2 (eIF2) by the guanine nucleotide exchange factor, eIF2B (see Fig. 1 A). eIF2 in its active GTP-bound form interacts with initiator methionyl tRNA (Met-tRNA$_i^{Met}$) to form a ternary complex (TC) (Hinnebusch, 2000). In yeast, this TC can associate with initiation factors eIF1, eIF3, and eIF5 to form the multifactor complex (MFC; Asano et al., 2000). The MFC recruits the 40S ribosomal subunit to the mRNA to allow subsequent scanning, recognition of the AUG start codon, and GTP hydrolysis on eIF2 (Hinnebusch, 2000). The conserved guanine nucleotide exchange factor eIF2B is required for recycling of the resulting GDP-bound eIF2 into the translationally active GTP-bound form. eIF2B is encoded in the yeast *Saccharomyces cerevisiae* by the essential genes *GCD1* (eIF2Bγ), *GCD2* (eIF2Bδ), *GCD6* (eIF2Bε), *GCD7* (eIF2Bβ), and the nonessential gene *GCN3* (eIF2Bα) (Hinnebusch, 2000). Mutations in the human genes encoding the five subunits of eIF2B have recently been identified as the cause of childhood ataxia with central nervous system hypomyelination also called leukoencephalopathy with vanishing white matter (van der Knaap et al., 2002). The eIF2B-dependent exchange reaction is a tightly regulated step in the translation initiation pathway. For instance, in mammalian cells, direct inhibition of eIF2B occurs in response to insulin signaling (Wang et al., 2001). In yeast, mutations in the γ subunit of eIF2B increase sensitivity to fusel alcohols such as butanol (Ashe et al., 2001). However, by far the best-characterized regulatory mechanism involves the phosphorylation of the α subunit of eIF2 on Ser-51. Phosphorylated eIF2 forms an inactive complex with eIF2B, resulting in a reduced cellular pool of active eIF2–GTP and hence a diminished rate of translation initiation (Hinnebusch, 2000). Four different mammalian eIF2α kinases have been identified, which are activated by different stresses (Dever, 2002). In contrast, in the yeast *S. cerevisiae*, the only eIF2α kinase is Gcn2p and studies of its regulation in response to amino acid starvation have served as a paradigm for other more complex systems (Hinnebusch, 2000).

In mammalian cells, stresses that promote eIF2α phosphorylation (e.g., arsenite or heat shock) result in the sequestration of mRNA and eukaryotic translation initiation factors into cytoplasmic granules, termed stress granules (Anderson and Kedersha, 2002; Kimball et al., 2003). These stress granules

Correspondence to Mark Ashe: mark.p.ashe@manchester.ac.uk

Abbreviations used in this paper: eIF, eukaryotic initiation factor; Met-tRNA$_i^{Met}$, initiator methionyl tRNA; MFC, multifactor complex; SCD, synthetic complete media; TC, ternary complex.

The online version of this article contains supplemental material.

The Journal of Cell Biology, Vol. 170, No. 6, September 12, 2005 925–934
http://www.jcb.org/cgi/doi/10.1083/jcb.200503162

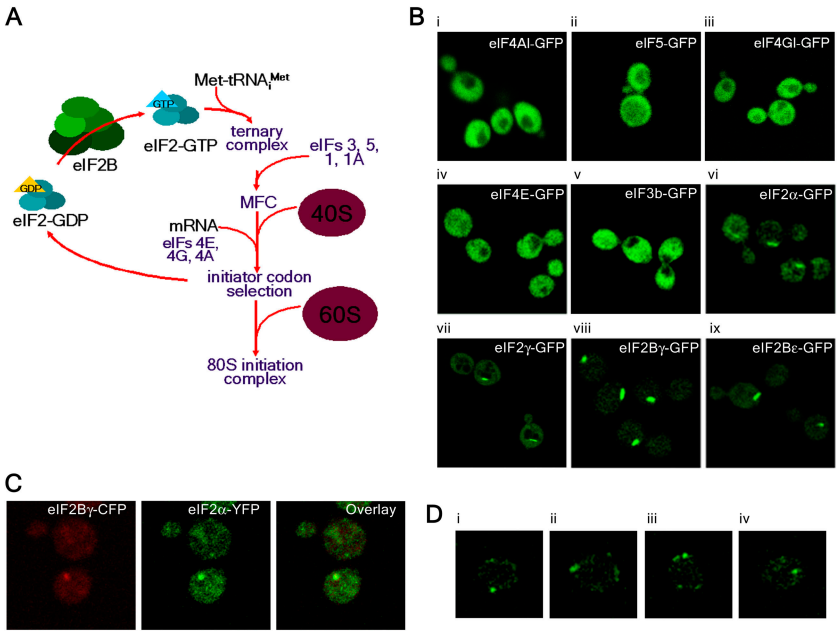

Figure 1. **Localization of eIFs in *S. cerevisiae*.** (A) Diagram representing the eukaryotic translation initiation pathway. (B) Live cell confocal microscopic images of strains YMK1170, 1171, 1172, 885, 881, 883, 1211, 880, and 882 bearing chromosomally integrated COOH-terminal eGFP tags, (i) *TIF1-GFP* (eIF4AI-GFP), (ii) *TIF5-GFP* (eIF5-GFP), (iii) *TIF4631-GFP* (eIF4GI-GFP), (iv) *CDC33-GFP* (eIF4E-GFP), (v) *PRT1-GFP* (eIF3b-GFP), (vi) *SUI2-GFP* (eIF2α-GFP), (vii) *GCD11-GFP* (eIF2γ-GFP), (viii) *GCD1-GFP* (eIF2Bγ-GFP), and (ix) *GCD6-GFP* (eIF2Bε-GFP). (C) Colocalization (left) *GCD1-CFP* (eIF2Bγ-GFP), (middle) *SUI2-YFP* (eIF2α-GFP), and (right, overlay) using strain YMK1144. (D) Immunofluorescence of fixed YMK467 cells with anti-eIF2Bε antibodies. Four defined images from the same field of view are shown.

have been proposed to be sites where mRNA is targeted to give untranslated mRNP complexes. In addition, mRNA decay factors in both mammalian cells and yeast have been demonstrated to aggregate into cytoplasmic foci (Sheth and Parker, 2003; Cougot et al., 2004). Intriguingly, in yeast these degradation factor foci (or P bodies) increase in response to stress (Teixeira et al., 2005).

In this paper we have assessed the localization of several key eukaryotic translation initiation factors in the yeast *S. cerevisiae*. We show that the guanine nucleotide exchange factor eIF2B and the guanine nucleotide binding protein eIF2 have a characteristic localization to a large cytoplasmic focus. This localization profile is both specific to these factors and dependent upon active protein synthesis. FRAP studies reveal that the eIF2 component continually shuttles between the foci and the cytoplasm whereas eIF2B is a stable feature of the foci. Several conditions known to inhibit eIF2B guanine nucleotide exchange prevent eIF2 shuttling into these foci. Therefore, we propose that these foci are sites of guanine nucleotide exchange and hence form part of a highly organized mechanism for regenerating translationally competent eIF2.

Results

In this study we have investigated the localization of eukaryotic translation initiation factors in yeast. The chromosomal copies of a number of yeast translation initiation factors were COOH-terminally tagged with the enhanced green fluorescent protein (eGFP) (Knop et al., 1999). These tagged proteins represent the sole source of the eIF in each yeast strain. The resultant tagged forms therefore support viability and present no discernable phenotype. In live cells, GFP-tagged eIF4AI, eIF5, eIF4GI, eIF4E, and eIF3b (Prt1p) are dispersed throughout the cytoplasm (Fig. 1 B, i, ii, iii, iv, and v). Conversely, the α and γ subunits of eIF2, and the γ and ε subunits of eIF2B, localize to a defined cytoplasmic focus, which is largely specific to the mother cell (Fig. 1 B, vi, vii, viii, and ix). This localization represents the site of 40.61% (±3.31) of eIF2Bγ factor localization, whereas only 17.50% (±1.32) of eIF2α localizes to the focus with the remainder showing diffuse cytoplasmic localization (Table I). To confirm the localization of the GFP-tagged forms, an indirect immunofluorescence assay using an antibody to the ε subunit of eIF2B was performed. This analysis confirmed the presence of the large cytoplasmic body observed with the GFP tagged proteins (Fig. 1 D).

eIF2B is the guanine nucleotide exchange factor for eIF2, and these factors are known to interact (Pavitt et al., 1998). Therefore, we examined whether eIF2 and eIF2B localize to the same cytoplasmic body within individual cells. A strain bearing eIF2α-YFP and eIF2Bγ-CFP was constructed and in this strain these proteins colocalize to the same cytoplasmic foci (Fig. 1 C).

The interaction of eIF2-GTP with Met-tRNA$_i^{Met}$ to form TC is a critical step in the translation initiation pathway (Hinnebusch, 2000). If the eIF2–eIF2B foci are sites of TC formation then Met-tRNA$_i^{Met}$ would be expected to colocalize. To address this, FISH analysis using a probe specific to Met-tRNA$_i^{Met}$ was performed. As a control, a probe to the elongator methionyl-tRNA was also used. As shown in Fig. 2 A, Met-tRNA$_i^{Met}$ does not colocalize to the sites of eIF2B localization. Therefore it seems unlikely that the localized foci represent sites of TC formation.

As determined by Western blot analysis, a basal level of phosphorylated eIF2α exists in yeast cells during non-stress conditions (Fig. 2 E). Previous studies have shown that phosphorylated eIF2 has a higher affinity for eIF2B (Pavitt et al., 1998). Therefore it is possible that the localized foci represent sites where this phosphorylated form of eIF2 is bound to eIF2B. To assess this we made use of a *gcn2Δ* strain, deficient

Table I. **Quantitation of the cellular distribution of eIF2 and eIF2B**

Strain	Growth conditions[a]	GFP-tagged protein	Percent of eIF2 or eIF2B in foci[b]
YMK880	Control	eIF2Bγ-GFP	40.61 ± 3.31
YMK880	−AA (15 min)	eIF2Bγ-GFP	55.45 ± 2.82[c]
YMK1087 (*gcn2Δ*)	Control	eIF2Bγ-GFP	43.39 ± 2.79
YMK1087 (*gcn2Δ*)	−AA (15 min)	eIF2Bγ-GFP	54.97 ± 1.40
YMK1180 eIF2Bε (WT)	Control	eIF2Bγ-GFP	43.48 ± 3.92
YMK1181 eIF2Bε (F250L)	Control	eIF2Bγ-GFP	42.27 ± 2.97
YMK883	Control	eIF2α-GFP	17.50 ± 1.32
YMK883	−AA (15 min)	eIF2α-GFP	36.46 ± 2.09[c]
YMK883	−AA (1 h)	eIF2α-GFP	32.02 ± 1.63
YMK1088 (*gcn2Δ*)	Control	eIF2α-GFP	20.93 ± 1.78
YMK1088 (*gcn2Δ*)	−AA (1 h)	eIF2α-GFP	18.95 ± 1.36
YMK883 + pRS316	Control	eIF2α-GFP	18.58 ± 2.67
YMK883 + pAV1245, *GCN2*[c]	Control	eIF2α-GFP	40.91 ± 2.23[c]
YMK883 + pAV1248, *GCN2*[c]	Control	eIF2α-GFP	40.62 ± 3.02[c]
YMK1168 eIF2Bε (WT)	Control	eIF2α-GFP	20.11 ± 4.39
YMK1169 eIF2Bε (F250L)	Control	eIF2α-GFP	20.42 ± 2.01

[a]Control. Cells were grown to exponential phase in SCD or SCD minus LEU at 30°C except in –AA, where all amino acids were removed for the indicated time.
[b]Using ImageJ software the total foci and cellular fluorescence was calculated, the background was subtracted, and the total eIF2 or eIF2B foci fluorescence was normalized to the total cellular fluorescence. The value shown represents the mean value calculated from ≥25 cells ± standard errors.
[c]When compared to the control sample the P value for each set was <0.05.

in the eIF2α kinase. As expected this strain contains no phosphorylated eIF2α under any conditions (Fig. 2 E). We observed no dramatic difference in the size or abundance of the localization of either the eIF2Bγ or the eIF2α subunits in the *gcn2*-null background strains in the presence or absence of amino acids as compared with the wild-type control (Fig. 2 B). A similar result is obtained when the γ subunit of eIF2 is GFP tagged and is observed in the presence of the nonphosphorylatable eIF2α (*SUI2 S51A*) (unpublished data). Therefore the localized eIF2–eIF2B foci do not solely represent sites where phosphorylated eIF2 sequesters eIF2B.

Intriguingly, although the overall localization of the eIF2 and eIF2B subunits is not altered in the wild-type cells during amino acid starvation, quantification of eIF2 in the foci after amino acid removal reveals an approximate twofold increase in eIF2α (Table I). The amino acid starvation conditions used are entirely comparable in terms of the level of eIF2α phosphorylation to the classically defined addition of 3-amino triazole (3-AT) (Fig. 2 E; Hinnebusch and Fink, 1983). As well as the twofold increase in eIF2α in the foci, these conditions also bring about a slight increase in eIF2Bγ. Interestingly, when eIF2 and eIF2B were quantified in the *gcn2*-null mutant the slight increase in eIF2B in the foci after amino acid starvation was still observed. However, under these conditions, there was no increase of eIF2 in the *gcn2*-null cells. The nonelevated level of eIF2 within the foci in the *gcn2Δ* strain was maintained even after an amino acid starvation of 1h. Therefore, although these foci are not dependent upon phosphorylated eIF2α, there is an increased level of eIF2 in the foci during stress which is not observed in a *gcn2*-null mutant. This may be a consequence of the reported increased affinity of phosphorylated eIF2 for eIF2B (Pavitt et al., 1998)

To assess whether these foci are integral features for active translation, we made use of the antibiotic cycloheximide. At concentrations of cycloheximide which inhibit both translation initiation and elongation (Arava et al., 2003), the eIF2–eIF2B foci are lost and the factors disperse throughout the cytoplasm (Fig. 2 C). Although cycloheximide inhibits the peptidyltransferase activity during translation elongation, the drug also inhibits translation initiation (Pestka, 1971; Arava et al., 2003). To investigate more specifically the importance of translation initiation on the localization of the eIF2–eIF2B foci we made use of the *prt1-1* mutation in the eIF3b subunit. Intriguingly, at the nonpermissive temperature this mutation also resulted in the dispersal of the eIF2–eIF2B foci (Fig. 2 D). It has recently been documented that in a *prt1-1* mutant at the nonpermissive temperature translation initiation is inhibited at a step upstream of eIF2 GTP hydrolysis and eIF2 is retained on the 40S ribosomal subunit (Nielsen et al., 2004). Therefore, it seems that either the maintenance of eIF2 bound to 40S subunits away from foci or the accumulation of GDP-bound eIF2 in the *prt1-1* mutant leads to disruption of the foci. This raises the question as to whether eIF2 is a required constituent of the foci and what the dynamics of the eIF2–eIF2B interaction are.

To examine the dynamic properties of these foci further, we made use of the technique FRAP. Using strains bearing either eIF2Bγ-GFP or eIF2α-GFP, the recovery of fluorescence was measured after targeted photobleaching of the eIF2–eIF2B foci. Photobleaching of the GFP chromophore is irreversible yet does not affect the function of proteins (White and Stelzer, 1999). Interestingly, after photobleaching eIF2α-GFP fluorescence in the foci rapidly recovers with a mean half time of recovery measuring $t_{1/2}$ = 3.63 s (±0.60) (Fig. 3, A and B). In contrast, recovery of eIF2Bγ-GFP was not observed over this

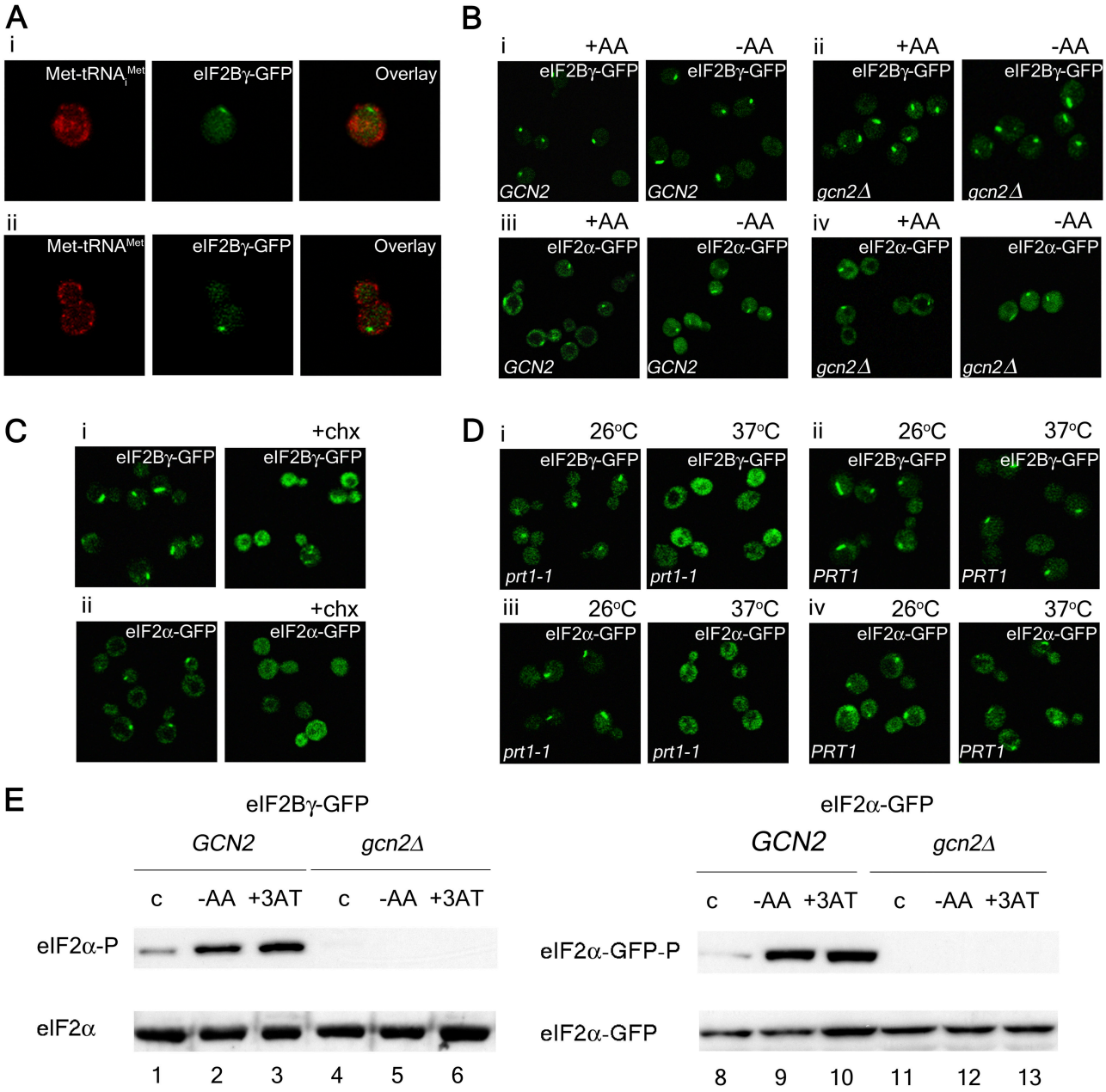

Figure 2. **The eIF2–eIF2B foci are not sites of eIF2B regulation or TC formation however they do require active translation.** (A) The localization of (i) initiator and (ii) elongator Met-tRNA^{Met} was analyzed in the eIF2Bγ-GFP–containing strain YMK880 by FISH using end-labeled oligonucleotides. FISH images were compared with eIF2Bγ-GFP localization in the overlay images. (B) *GCN2* and *gcn2*-null strains bearing eIF2Bγ-GFP, YMK880 (i) and YMK1087 (ii), and eIF2α-GFP, YMK883 (iii), and YMK1088 (iv) were grown in media containing (+AA) or lacking amino acids (−AA) for 15 min. Cells were visualized by live cell confocal microscopy. (C) Strains YMK880 (i, eIF2Bγ-GFP) and YMK883 (ii, eIF2α-GFP) were incubated at room temperature for 10 min in the presence or absence of cycloheximide (100 μg/ml). (D) The strains (i) YMK1123 (eIF2Bγ-GFP, *prt1-1*), (ii) YMK880 (eIF2Bγ-GFP), (iii) YMK1124 (eIF2α-GFP, *prt1-1*), and (iv) YMK883 (eIF2α-GFP) were incubated at the permissive (26°C) and nonpermissive (37°C) temperature for 15 min. Cells were visualized by live cell confocal microscopy. (E) Protein extracts from eIF2Bγ-GFP strains YMK880 (*GCN2*, lanes 1–3), YMK1087 (*gcn2Δ*, lanes 4–6), and eIF2α-GFP strains, YMK883 (*GCN2*, lanes 8–10), and YMK1088 (*gcn2Δ*, lanes 11–13) were blotted and probed with antibodies to eIF2α and phospho-specific antibodies to phosphoserine 51 on eIF2α.

time period (Fig. 3, C and D). Detailed images of representative FRAP experiments are shown in Fig. S1 (available at http://www.jcb.org/cgi/content/full/jcb.200503162/DC1). These results suggest that eIF2 is rapidly shuttling into the foci while the guanine nucleotide exchange factor eIF2B is a resident feature. This raises the possibility that guanine nucleotide exchange might be occurring directly in these foci.

Amino acid starvation is a well documented stress in yeast, which reduces the guanine nucleotide exchange rate of reaction for eIF2B. Visualization of the eIF2B- and eIF2-tagged proteins upon removal of amino acids does not reveal an alteration in the localization of the eIF2–eIF2B foci, however, the proportion of eIF2α in the foci does increase upon the removal of amino acids (Fig. 2 B and Table I). FRAP analysis

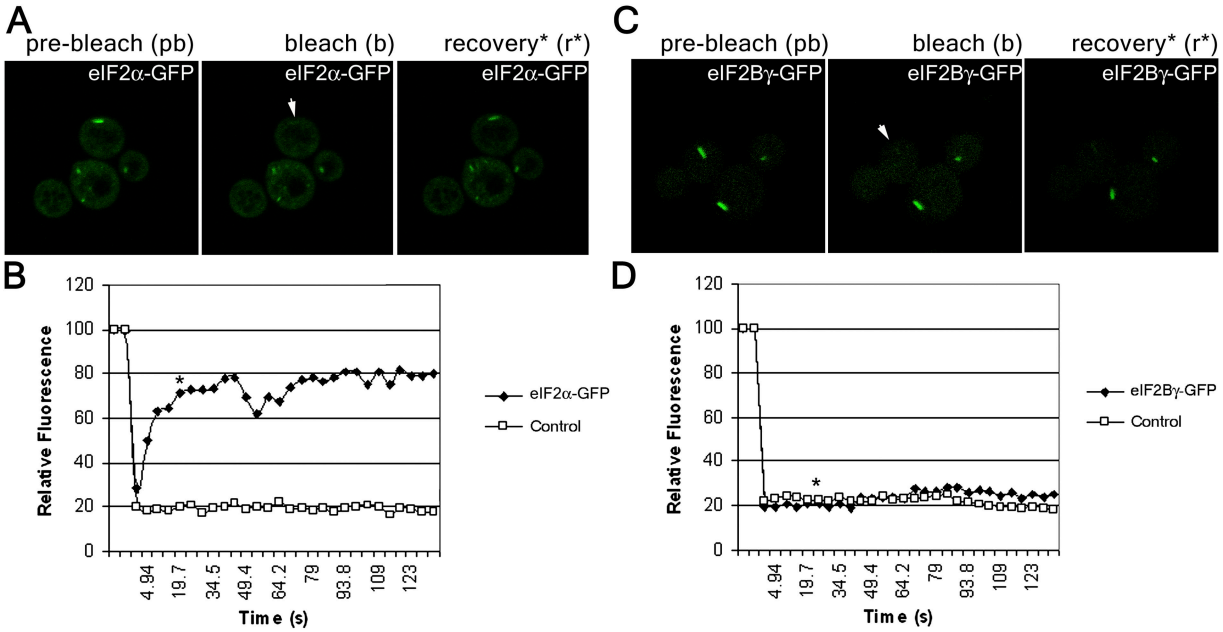

Figure 3. **eIF2 cycles rapidly through the foci whereas eIF2B is less dynamic.** (A) eIF2α-GFP FRAP analysis. Panels show representative prebleach (pb), bleach (b), and recovery (r) images from FRAP experiment on strain YMK883. The bleached focus is marked with a white arrowhead and the asterisk on the recovery image corresponds to time point on the graph when the image was taken. (B) Graph show quantitation of eIF2α-GFP FRAP experiments. Control represents the FRAP results from YMK883 fixed cells. (C) eIF2Bγ-GFP FRAP analysis. Panels show representative prebleach (pb), bleach (b), and recovery (r) images from FRAP experiment on strain YMK880. The bleached focus is marked with a white arrowhead and the asterisk on the recovery image corresponds to time point on the graph when the image was taken. (D) Graph show quantitation of eIF2Bγ-GFP FRAP experiments. Control represents the FRAP results from YMK880-fixed cells.

shows that upon removal of amino acids there is a significant reduction in the mean rate of recovery for eIF2α-GFP, $t_{1/2}$ = 13.45 s (±1.87; Fig. 4, A and B). The three- to fourfold change in FRAP recovery is consistent with the change in rate of protein synthesis observed after amino acid starvation (unpublished data). Therefore a condition known to inhibit the guanine nucleotide exchange activity of eIF2B, leads to a reduced rate of eIF2 shuttling into the foci. Longer time points of amino acid starvation (e.g., 1 h), exacerbated the reduction of eIF2 recycling (Fig. 4, C and D). Interestingly, when FRAP experiments using a *gcn2Δ* strain (which is translationally resistant to amino acid starvation as eIF2α cannot be phosphorylated) were performed after amino acid starvation, eIF2α recovery after photobleaching is unaffected where the $t_{1/2}$ = 3.35 s (±0.29; Fig. 4, C and D).

To further investigate the hypothesis that these foci could represent specific sites of eIF2B guanine nucleotide exchange activity, we used two alternative strategies to inhibit eIF2B activity. First, we monitored the rate of eIF2 recovery in eIF2α-GFP–bearing strains, harboring plasmids containing the constitutive *GCN2* alleles (*GCN2^c*), pAV1245 [*GCN2^c*M788V-E1606G], and pAV1248 [*GCN2^c*M788V-E1591K] (Ramirez et al., 1992; Garcia-Barrio et al., 2000). In these strains, the dominant activation of Gcn2p kinase leads to constitutive eIF2α phosphorylation and thus decreased eIF2B activity. This increase in eIF2α phosphorylation is shown by Western blot analysis in Fig. 5 C where both constitutive alleles of Gcn2p result in equivalent levels of eIF2α phosphorylation to those observed under the classically defined amino acid starvation conditions (Hinnebusch and Fink, 1983). In the presence of both mutant alleles little recovery of eIF2 fluorescence was observed after photobleaching. In addition, the fraction of eIF2 in the foci is elevated over twofold relative to wild type, consistent with the elevated eIF2α phosphorylation and the increase in the fraction of eIF2 in the foci after amino acid starvation (Fig. 5 C and Table I). Therefore increasing the level of eIF2α phosphorylation reduces the rate of eIF2 shuttling through the foci. Second, we made use of a strain bearing a point mutation in the ε subunit of eIF2B (*gcd6-F250L),* to test eIF2 recovery after photobleaching (Gomez and Pavitt, 2000). This strain is also deleted for the eIF2 kinase Gcn2p, which ensures that the effect on eIF2 is purely a result of altered eIF2B activity and not a result of potential phosphorylation of eIF2 by Gcn2p. As for the constitutive *GCN2* alleles, the eIF2 foci failed to recover after photobleaching in this eIF2B mutant strain whereas for the wild-type controls eIF2α-GFP foci recovered normally (Fig. 5, D and E). Therefore an eIF2B mutant with reduced guanine nucleotide exchange activity shows a greatly reduced rate of eIF2 shuttling through the foci.

Discussion

In this study we show that eIF2 and eIF2B colocalize to a specific focus within the cell, whereas other translation initiation factors show a dispersed cytoplasmic localization. Our data support the hypothesis that these eIF2–eIF2B foci are sites where guanine nucleotide exchange occurs. First, both eIF2

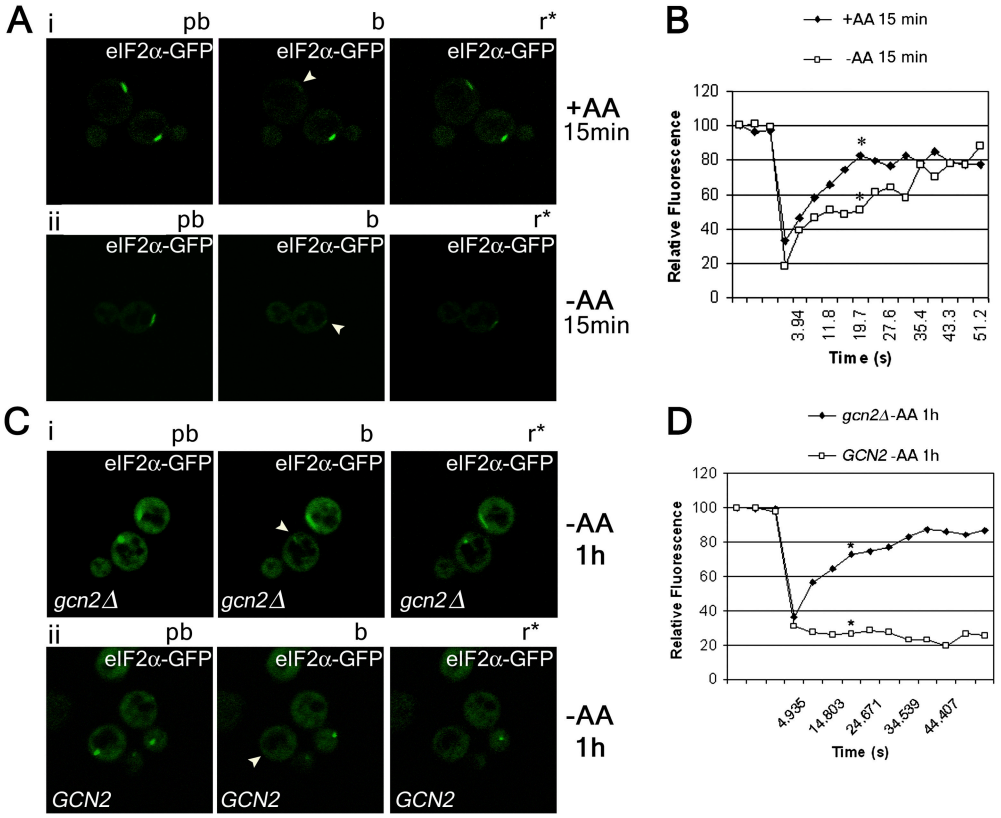

Figure 4. **eIF2α-GFP shuttling is altered in the absence of amino acids.** Figure shows FRAP experiments on eIF2α-GFP–bearing strains as described in Fig. 3. (A) YMK883 FRAP after (i) 15-min control incubation and (ii) 15-min starvation for amino acids. (B) Graph showing quantitation of eIF2α-GFP amino acid starvation FRAP experiments. (C) YMK1088 (i, *gcn2Δ*) and (ii) YMK883 strains after 1 h starvation for amino acids. (D) Graph showing quantitation of eIF2α-GFP FRAP experiments after a 1-h amino acid starvation in the presence and absence of Gcn2p. pb, Prebleach; b, bleach; and r, recovery.

(the guanine nucleotide binding protein) and eIF2B (the guanine nucleotide exchange factor for eIF2) localize to the same foci in actively growing and translating cells. Second, eIF2 has the ability to rapidly shuttle into and out of these foci, whereas eIF2B is a more stable component. Moreover, three independent means of inhibiting eIF2B activity all result in reduced eIF2 shuttling (Table II). Therefore, these combined results suggest that eIF2 dynamically migrates through a center for guanine nucleotide exchange.

Interestingly, the integrity of these foci requires active translation, as cycloheximide an antibiotic that inhibits both translation initiation and translation elongation, disrupts the localization of the eIF2–eIF2B foci. The localization of the two factors is also disrupted in the presence of the eIF3b mutant, *prt1-1*. These results are surprising and pose the question, why would the inhibition of translation initiation disperse a focused center of the guanine nucleotide exchange factor, eIF2B? From the quantification data we know that stresses that increase the level of phosphorylated eIF2α and thereby decrease the guanine nucleotide exchange activity, do not alter the structure of the foci but rather increase the proportion of eIF2 localizing to the foci (Table I). This is intriguing with respect to the cycloheximide result as in mammalian systems work has documented that the addition of cycloheximide induces the phosphorylation of eIF2α thereby sequestering eIF2B activity (Jiang et al., 2003). We have performed Western analysis under the cycloheximide conditions used to inhibit translation in yeast and do not see any increase in the level of phosphorylated eIF2α (unpublished data). We favor the idea that the addition of cycloheximide results in the dispersal of the eIF2–eIF2B guanine nucleotide exchange body by preventing the flux of eIF2 through the foci. We envisage that the sequestration of eIF2 on the ribosome or the accumulation of eIF2 in a GTP-bound form might limit eIF2 dynamics through the foci. This theory is supported by a similar dispersal of the foci in the presence of a *prt1-1* mutant. Recent data suggests that in a *prt1-1* mutant, eIF2 is sequestered in 48S preinitiation complexes and translation initiation is inhibited at a step upstream of eIF2 GTP hydrolysis (Nielsen et al., 2004). Therefore, in this mutant accumulation of GTP-bound eIF2 or eIF2 bound to ribosomes would limit the availability of GDP-bound eIF2. This interpretation suggests that the eIF2–eIF2B foci are sensitive to the level of GDP-bound eIF2 and if this falls below a defined threshold the foci disperse.

Another obvious question is whether these foci relate to the mammalian cytoplasmic stress granules or the processing bodies containing mRNA decay factors (Anderson and Kedersha, 2002; Sheth and Parker, 2003). The mammalian stress granules contain many translation initiation factors in stalled

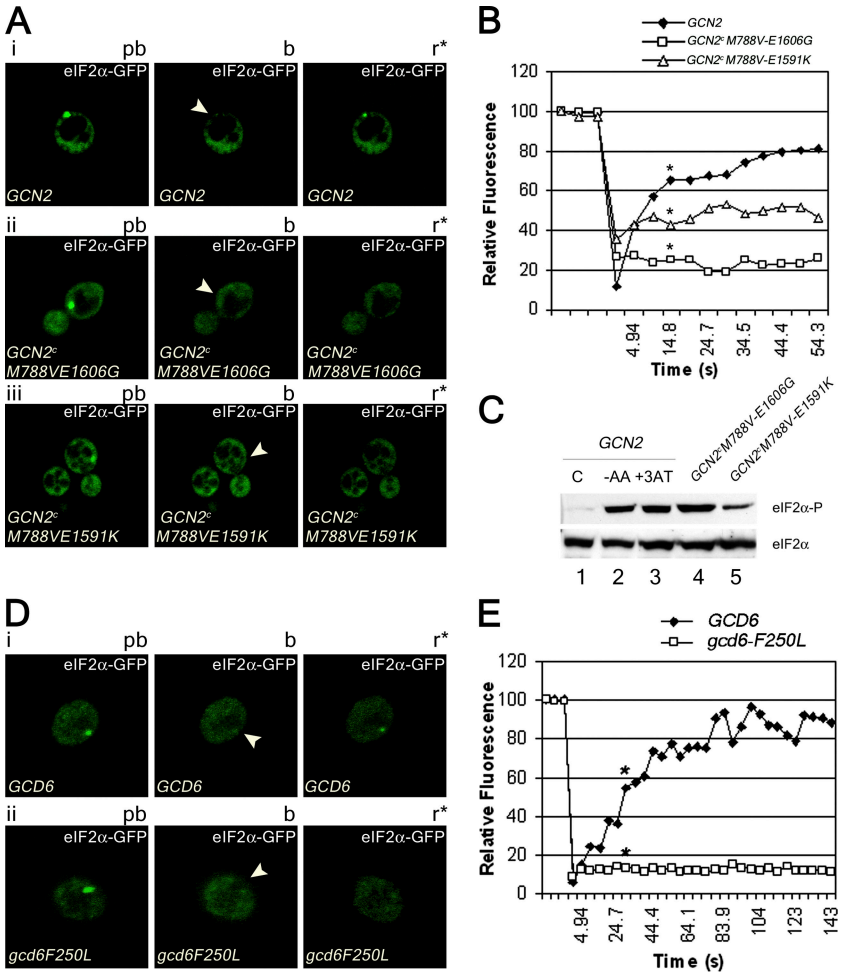

Figure 5. **The eIF2–eIF2B foci represent sites of guanine nucleotide exchange.** Figure shows FRAP experiments on eIF2α-GFP bearing strains as described in Fig. 3. (A) YMK883 strains transformed with (i) control plasmid, pRS316, (ii) pAV1245 (*GCN2*^{c}M788V-E1606G), and (iii) pAV1248 (*GCN2*^{c}M788-E1591K), respectively. (B) Graph showing quantitation of eIF2α-GFP FRAP experiments with *GCN2*^{c} mutants. (C) Protein extracts from strains YMK883 pRS316, YMK883 pAV1245[*GCN2*^{c}M788V-E1606G], and YMK883 pAV1248[*GCN2*^{c}M788V-E1591K] were blotted and probed with antibodies to eIF2α and phosphospecific antibodies to phophoserine 51 on eIF2α. (D) FRAP analysis of eIF2α-GFP in strains (i) YMK1168 (*GCD6*) and (ii) YMK1169 (*gcd6-F250L*). (E) Graph showing quantitation of eIF2α-GFP FRAP experiments with wt and eIF2Bε catalytic mutant. pb, Prebleach; b, bleach; r, recovery.

complexes (Anderson and Kedersha, 2002; Kimball et al., 2003). The yeast foci described here probably serve distinct functions as they are not dependent upon stress, they do not contain eIF3, eIF4G, or eIF4E, and are unchanged in an eIF2α kinase mutant. Recent work has demonstrated that the yeast mRNA decay factors localize to cytoplasmic processing bodies (Sheth and Parker, 2003). The eIF2–eIF2B foci are distinct from these processing bodies as they localize to unrelated cytoplasmic regions (unpublished data). Indeed processing bodies like the mammalian stress granules become more pronounced and abundant under translationally inhibited conditions (Teixeira et al., 2005), yet the eIF2–eIF2B foci are associated with highly active translation initiation and are dispersed after complete inhibition of translation initiation.

If these foci represent sites of guanine nucleotide exchange then it is possible that the in vivo rate of eIF2 shuttling and level of eIF2 associated with the foci can be informative

Table II. $t_{1/2}$ **values for FRAP experiments**

Strain	Growth conditions[a]	GFP-tagged protein	Mean $t_{1/2}$ recovery[b] (s)
YMK880	Control	eIF2Bγ-GFP	RI
YMK883	Control	eIF2α-GFP	3.63 ± 0.60
YMK883	−AA (15 min)	eIF2α-GFP	13.45 ± 1.87
YMK883	−AA (1 h)	eIF2α-GFP	RI
YMK1088 (*gcn2Δ*)	−AA (1 h)	eIF2α-GFP	3.35 ± 0.29
YMK883 + pRS316	Control	eIF2α-GFP	3.66 ± 0.36
YMK883 + pAV1245, *GCN2*^{c}	Control	eIF2α-GFP	RI
YMK883 + pAV1248, *GCN2*^{c}	Control	eIF2α-GFP	17.31 ± 2.30
YMK1168 eIF2Bε (wt)	Control	eIF2α-GFP	4.35 ± 0.63
YMK1169 eIF2Bε (F250L)	Control	eIF2α-GFP	RI

[a]Control. Cells were grown to exponential phase in SCD or SCD minus LEU at 30°C except in –AA, where all amino acids were removed for the indicated time.
[b]Mean value was calculated from at least 10 different FRAP experiments. The values are shown ± the standard error.
RI, recovery insufficient for $t_{1/2}$ measurement.

with regard to the kinetics and dynamics of the exchange reaction (Nika et al., 2000). When yeast cells are starved for amino acids the α subunit of eIF2 is phosphorylated and as a consequence the affinity of eIF2 for eIF2B increases (Pavitt et al., 1998). This tight binding of phosphorylated eIF2 to eIF2B results in a decreased rate of nucleotide exchange under limiting eIF2B levels (Sudhakar et al., 2000). When the level of eIF2 in the foci was quantified we observed an increase after amino acid starvation (Table I). That this increase is due to the phosphorylation of the eIF2α subunit is demonstrated as it is not observed in a *gcn2*-null mutant under the same stress conditions. FRAP analysis measures the recovery of fluorescence into the foci and could therefore relate to the rate at which eIF2-GDP enters the exchange region (i.e., the on rate). Therefore, the decreased rate of eIF2 shuttling observed by FRAP may be a consequence of a decreased off rate due to the increased affinity of phosphorylated eIF2 for eIF2B. This interpretation is further supported by experiments using *GCN2*-constitutive mutants. Here the constitutive level of phosphorylated eIF2α as determined by Western blot analysis is comparable to the level obtained after amino acid starvation and as a consequence dramatic reduction in shuttling is observed (Fig. 5, B and C).

The FRAP and quantification analyses for the exchange mutant of eIF2B are intriguing. This mutant results in no recovery of eIF2 fluorescence after photobleaching, which is consistent with previous decreased exchange activity for this mutant (Gomez and Pavitt, 2000). However, the quantification data reveals no increase in the level of eIF2 in the foci for this mutant. This lack of increased eIF2 binding is consistent with previous in vitro work where no difference in affinity for eIF2 was observed for this mutant (Gomez and Pavitt, 2000). These data suggest that for this mutant there is a decrease in both the association to and dissociation from eIF2B in the foci, and that this may relate to a decrease in both the on and off rate with regard to guanine nucleotide exchange.

From the quantification data we observed that only 40% of eIF2B localizes to the foci. Although we propose that this is a site where guanine nucleotide exchange takes place it is almost certainly not the sole site for exchange in the cell and other pools of eIF2B-dependent guanine nucleotide exchange are likely to exist. Indeed, there is evidence to suggest that some exchange may take place on the ribosome (Ramaiah et al., 1992).

Guanine nucleotide exchange by eIF2B, results in the regeneration of active eIF2-GTP from inactive eIF2-GDP. This exchange reaction is fundamental for the efficient regulation of translation initiation in response to many stresses. It is known that the total cellular level of eIF2 complexes far exceeds the cellular level of eIF2B (von der Haar and McCarthy, 2002). It is therefore intriguing to speculate that for extremely efficient guanine nucleotide exchange to take place, the cell may need to concentrate eIF2B into a defined region of the cell. In doing so, the eIF2 molecules must shuttle to and from this region in order to exchange their guanine nucleotides. Additionally, as eIF2B is a target for the inhibition of translation initiation, a localized region of complexes may augment this regulation.

Materials and methods

Strains construction and growth conditions

Yeast strains (Table III) were grown on standard yeast extract, peptone, glucose (YPD) media, or synthetic complete media (SCD) at 30°C (Guthrie and Fink, 1991). Amino acid starvation was brought about by the removal of all amino acids for 15 min. Strains were COOH-terminally tagged with eGFP, CFP, or YFP using a PCR-based assay and plasmids pYM12, pYM31, and pYM797 (Dr. G. Pereira, The University of Manchester, Manchester, UK; Knop et al., 1999). The GFP tagging was confirmed by both PCR and Western blot analysis. The strains YMK807 and YMK467 were generated by transformation of strains YMK23 and YMK36 with an *ADE2* DNA fragment. YMK1123 and YMK1124 were generated by crossing YMK135 with YMK880 and YMK883, respectively. Strains YMK1087 and YMK1088 were generated by crossing YMK515 with YMK880 and YMK883, respectively. Strains YMK1212 and YMK1213 were constructed by crossing YMK127 and YMK1211 and YMK129 and YMK1211, respectively.

Microscopy and FRAP analysis

GFP microscopy and FRAP analysis were performed using live cells grown in SCD media. The cells were mounted onto 0.5% poly-L-lysine–coated slides and visualized on a Zeiss LSM 510 confocal microscope with a 100× Plan Apochromat oil objective (NA 1.4). An argon laser (488 nm) was used at 55% capacity and the images were analyzed with Zeiss LSM software (Carl Zeiss MicroImaging, Inc.). For FRAP analysis the highest value of three initial prebleached images was set to 100% intensity. A defined region around the foci was chosen as the bleached area. Photobleaching was performed at 100% laser transmission and recovery was followed by recording images at 5 s intervals after bleaching at 4% laser transmission. Each image is composed of an average of three scans. Control cells were fixed in 3.7% formaldehyde for 1 h before FRAP analysis. Data analysis and the $\tau_{1/2}$ values (the time needed to reach half of the final intensity after bleaching) were generated as previously described (Rabut and Ellenberg, 2005). Quantification of the eIF2 and eIF2B foci was performed using the National Institutes of Health ImageJ software. The significance of variability amongst the means of the experimental groups shown in Table I was determined by paired test, using PRISM® Version 4 software (GraphPAD Software). Differences among experimental groups were considered to be statistically significant when $P < 0.05$. The images were compiled using Adobe Photoshop software (version 7.0).

Indirect immunofluorescence

Cells were fixed in 3.7% formaldehyde left at room temperature for 1 h and pelleted. Cell pellets were washed in 0.1 M potassium phosphate, pH 7.5, resuspended in 1 mg/ml lyticase, 0.1 M potassium phosphate, pH 7.5, and incubated a 30°C for 30 min. The resulting spheroplasts were gently pelleted, resuspended in PBS, and mounted onto 0.1% (wt/vol) poly-L-lysine–coated slides. Cells were blocked for 30 min in 4% BSA, PBS in a humid chamber, and then incubated with primary antibody anti-eIF2Bε (provided by Dr. G Pavitt, The University of Manchester) overnight at 4°C. After a number of washes in PBS the cells were incubated with an anti–rabbit secondary antibody for 2 h in the dark. Cells were washed with PBS and mounted in mounting solution (1 mg/ml phenylenediamine, 90% glycerol, 50 mM Tris, pH 9.0, 50 ng/ml DAPI). The cells were viewed using a 100× Plan Apochromat oil objective (NA 1.4). An argon laser (488 nm) was used at 55% capacity and the images were analyzed with Zeiss LSM software (Carl Zeiss MicroImaging, Inc.).

Western blot analysis of eIF2α and phosphoserine 51 eIF2α

Yeast strains were grown to an OD_{600} of 0.7 in SCD-His and treated in the absence of amino acids or the presence of 50 mM 3-aminotriazole (3-AT) for 15 min as described previously (Holmes et al., 2004). Yeast strains containing the *GCN2*^{c} mutant plasmids were grown to an OD_{600} of 0.7 in SCD-Ura. All cells were lysed and protein samples were prepared, electrophoretically separated, and subjected to immunoblot analysis as described previously (Ashe et al., 2000). The phosphospecific eIF2α (Biosource International) and eIF2α (provided by Dr. G. Pavitt) antibodies were used for the detection.

FISH of tRNA

FISH was carried out as previously described (Sarkar and Hopper, 1998). Oligonucleotide probes were labeled at their 3′ end using terminal trans-

Table III. **Strains used in this study**

Name	Genotype	Source
YMK23	*MATa, ade2-1, his3-11,15, leu2-3, 112, trp1-1, ura3-1, can1-100, GCD1-P180*	(Ashe et al., 2001)
YMK36	*MATa, ade2-2, his3-11, 15, leu2-3, 112, trp1-1, ura3-1, can1-100 GCD1-S180*	(Ashe et al., 2001)
YMK807	*MATa, ADE2, his3-11, 15, leu2-3, 112, trp1-1, ura3-1, can1-100, GCD1-S180*	This study
YMK467	*MATα, ADE2, his3-11, 15, leu2-3, 112, trp1-1, ura3-1, can1-100, GCD1-P180*	This study
YMK880	*MATα, ADE2, his3-11, 15, leu2-3, 112, trp1-1, ura3-1, can1-100, GCD1-P180-GFP::G418*	This study
YMK881	*MATα, ADE2, his3-11, 15, leu2-3, 112, trp1-1, ura3-1, can1-100, GCD1-P180, PRT1-GFP::G418*	This study
YMK882	*MATα, ADE2, his3-11, 15, leu2-3, 112, trp1-1, ura3-1, can1-100, GCD1-P180 GCD6-GFP::G418*	This study
YMK883	*MATα, ADE2, his3-11, 15, leu2-3, 112, trp1-1, ura3-1, can1-100, GCD1-P180 SUI2-GFP::G418*	This study
YMK885	*MATα, ADE2, his3-11, 15, leu2-3, 112, trp1-1, ura3-1, can1-100, GCD1-P180 CDC33-GFP::G418*	This study
YMK1170	*MATα, ADE2, his3-11, 15, leu2-3, 112, trp1-1, ura3-1, can1-100, GCD1-P180 TIF1-GFP::G418*	This study
YMK1171	*MATα, ADE2, his3-11, 15, leu2-3, 112, trp1-1, ura3-1, can1-100, GCD1-P180 TIF5-GFP::G418*	This study
YMK1172	*MATα, ADE2, his3-11, 15, leu2-3, 112, trp1-1, ura3-1, can1-100, GCD1-P180 TIF4631-GFP::G418*	This study
YMK515	*MATa, ade2-1, HIS3, leu2-3, 112, trp1-1 ura3-1, can1-100, GCD1-P180, gcn2::URA3*	(Ashe et al., 2001)
YMK1087	*MATa, ADE2, HIS3, leu2-3, 112, trp1-1, ura3-1, can1-100, GCD1-P180-GFP::G418, gcn2::URA3*	This study
YMK1088	*MATa, ADE2, HIS3, leu2-3, 112, trp1-1, ura3-1, can1-100, GCD1-P180 gcn2::URA3, SUI2-GFP::G418*	This study
YMK135	*MATa, ade2-1, HIS3, leu2-1, 11, trp1-1, ura3-1, can1-100, prt1-1*	Ashe strain collection
YMK1123	*MATa, ADE2, his3-11, 15, leu2-3, 112, trp1-1, ura3-1, can1-100, prt1-1, GCD1-GFP::G418*	This study
YMK1124	*MATa, ADE2, his3-11, 15, leu2-3, 112, trp1-1, ura3-1, can1-100, prt1-1, SUI2-GFP::G418*	This study
YMK1144	*MATa, ADE2, his3-11, 15, leu2-3, 112, trp1-1, ura3-1, can1-100, GCD1-CFP::HIS, SUI2-YFP::HIS*	This study
YMK1168	*MATα leu2-3, 112, ura3-52::[HIS4-lacZ ura3-52] ino1, gcd6Δ, gcn2Δ::hisG, SUI2-GFP::G418, p[GCD6 CEN6 LEU2]*	This study
YMK1169	*MATα leu2-3, 112, ura3-52::[HIS4-lacZ ura3-52] ino1, gcd6Δ, gcn2Δ::hisG, SUI2-GFP::G418, p[gcd6-F250L CEN6 LEU2]*	This study
YMK1180	*MATα leu2-3, 112, ura3-52::[HIS4-lacZ ura3-52] ino1, gcd6Δ, gcn2Δ::hisG, GCD1-GFP::G418, p[GCD6 CEN6 LEU2]*	This study
YMK1181	*MATα leu2-3, 112, ura3-52::[HIS4-lacZ ura3-52] ino1, gcd6Δ, gcn2Δ::hisG, GCD1-GFP::G418, p[gcd6-F250L CEN6 LEU2]*	This study
YMK1211	*MATα, ADE2, his3-11, 15, leu2-3, 112, trp1-1, ura3-1, can1-100, GCD1-P180, GCD11-GFP::G418*	This study
YMK1212	*MATα, ADE2, his3-11, 15, leu2-3, 112, trp1-1, ura3-1, can1-100, GCD1-P180, sui2Δ, GCD11-GFP::G418, p[SUI2-S51A LEU CEN]*	This study
YMK1213	*MATα, ADE2, his3-11, 15, leu2-3, 112, trp1-1, ura3-1, can1-100, GCD1-P180, sui2Δ, GCD11-GFP::G418, p[SUI2 LEU CEN]*	This study
YMK127	*MATa, ADE2, his3-11, 15, leu2-3, 112, trp1-1, ura3-1, can1-100, GCD1-P180, sui2Δ, p[SUI2-S51A LEU CEN]*	Ashe strain collection
YMK129	*MATa, ADE2, his3-11, 15, leu2-3, 112, trp1-1, ura3-1, can1-100, GCD1-P180 sui2Δ, p[SUI2 LEU CEN]*	Ashe strain collection

ferase and digoxigenin-11-UTP according to manufacturer's recommendations (Roche Pharmaceuticals).

Online supplemental material

Fig. S1 shows individual recovery images from FRAP analysis of eIF2α-GFP and eIF2Bγ-GFP in Fig. 3. Online supplemental material is available at http://www.jcb.org/cgi/content/full/jcb.200503162/DC1.

We thank G. Pereira, G. Pavitt, and C. Stirling for reagents and advice. We thank D. Jackson and C. Tang for their assistance with the confocal microscopy. We especially thank R. Parker and D. Teixeira for helpful discussion.

This work and S.G. Campbell was supported by a Wellcome Trust project grant 067328/Z/02/Z to M.P. Ashe. N.P. Hoyle was supported by a Biotechnology and Biological Sciences Research Council strategic studentship.

Submitted: 29 March 2005
Accepted: 3 August 2005

References

Anderson, P., and N. Kedersha. 2002. Stressful Initiations. *J. Cell Sci.* 115: 3227–3234.

Arava, Y., Y. Wang, J.D. Storey, C.L. Liu, P.O. Brown, and D. Herschlag. 2003. Genome-wide analysis of mRNA translation profiles in *Saccharomyces cerevisiae*. *Proc. Natl. Acad. Sci. USA.* 100:3889–3894.

Asano, K., J. Clayton, A. Shalev, and A.G. Hinnebusch. 2000. A multifactor complex of eukaryotic initiation factors eIF1, eIF2, eIF3, eIF5 and initiator $tRNA^{Met}$ is an important translation initiation intermediate in vivo. *Genes Dev.* 14:2534–2546.

Ashe, M.P., S.K. De Long, and A.B. Sachs. 2000. Glucose depletion rapidly inhibits translation initiation in yeast. *Mol. Biol. Cell.* 11:833–848.

Ashe, M.P., J.W. Slaven, S.K. De Long, S. Ibrahimo, and A.B. Sachs. 2001. A novel eIF2B-dependent mechanism of translational control in yeast as a response to fusel alcohols. *EMBO J.* 20:6464–6474.

Cougot, N., S. Babajko, and B. Seraphin. 2004. Cytoplasmic foci are sites of mRNA decay in human cells. *J. Cell Biol.* 165:31–40.

Dever, T.E. 2002. Gene-specific regulation by general translation factors. *Cell.* 108:545–556.

Garcia-Barrio, M., J. Dong, S. Ufano, and A.G. Hinnebusch. 2000. Association of GCN1-GCN20 regulatory complex with the N-terminus of eIF2α kinase GCN2 is required for GCN2 activation. *EMBO J.* 19:1887–1899.

Gomez, E., and G.D. Pavitt. 2000. Identification of domains and residues within the ε subunit of eukaryotic translation initiation factor 2B (eIF2Bε) required for guanine nucleotide exchange reveals a novel activation function promoted by eIF2B complex formation. *Mol. Cell. Biol.* 20:3965–3976.

Guthrie, C., and G.R. Fink. 1991. Guide to Yeast Genetics and Molecular Biology. Academic Press, San Diego, CA. 933 pp.

Hinnebusch, A.G. 2000. Mechanism and regulation of initiator methionyl-tRNA binding to ribosomes. *In* Translational Control of Gene Expression. N. Sonenberg, J.W. Hershey, and M. Mathews, editors. Cold Spring Harbor Laboratory Press, Cold Spring Harbor, NY. 185–244.

Hinnebusch, A.G., and G.R. Fink. 1983. Positive regulation in the general amino acid control of *Saccharomyces cerevisiae*. *Proc. Natl. Acad. Sci. USA.* 80:5374–5378.

Holmes, L.E.A., S.G. Campbell, S.K. De Long, A.B. Sachs, and M.P. Ashe. 2004. Loss of translational control in yeast compromised for the major mRNA decay pathway. *Mol. Cell. Biol.* 24:2998–3010.

Jiang, H.-Y., S.A. Wek, B.C. McGrath, D. Scheuner, R.J. Kaufman, D.R. Cavener, and R.C. Wek. 2003. Phosphorylation of the α subunit of eukaryotic initiation factor 2 is required for activation of NF-κB in response to diverse cellular stresses. *Mol. Cell. Biol.* 23:5651–5663.

Kimball, S.R., R.L. Horetsky, D. Ron, L.S. Jefferson, and H.P. Harding. 2003. Mammalian stress granules represent sites of accumulation of stalled translation initiation complexes. *Am. J. Physiol. Cell Physiol.* 284:C273–C284.

Knop, M., K. Siegers, G. Pereira, W. Zachariae, B. Winsor, K. Nasmyth, and E. Schiebel. 1999. Epitope tagging of yeast genes using a PCR-based strategy: more tags and improved practical routines. *Yeast.* 15:963–972.

Nielsen, K.H., B. Szamecz, L. Valasek, A. Jivotovskaya, B.S. Shin, and A.G. Hinnebusch. 2004. Functions of eIF3 downstream of 48S assembly impact AUG recognition and *GCN4* translational control. *EMBO J.* 23:1166–1177.

Nika, J., W. Yang, G.D. Pavitt, A.G. Hinnebusch, and E.M. Hannig. 2000. Purification and kinetic analysis of eIF2B from *Saccharomyces cerevisiae*. *J. Biol. Chem.* 275:26011–26017.

Pavitt, G.D., K.V.A. Ramaiah, S.R. Kimball, and A.G. Hinnebusch. 1998. eIF2 independently binds two distinct eIF2B subcomplexes that catalyze and regulate guanine-nucleotide exchange. *Genes Dev.* 12:514–526.

Pestka, S. 1971. Inhibitors of ribosome functions. *Annu. Rev. Microbiol.* 25: 487–562.

Rabut, G., and J. Ellenberg. 2005. Photobleaching techniques to study mobility and molecular dynamics of proteins in live cells: FRAP, iFRAP and FLIP. *In* Live Cell Imaging: A Laboratory Manual. R.D. Goldman and D.L. Spector, editors. Cold Spring Harbor Laboratory Press, Cold Spring Harbor, NY. 101–126.

Ramaiah, K.V., R.S. Dhindsa, J.-J. Chen, I.M. London, and D. Levin. 1992. Recycling and phosphorylation of eukaryotic initiation factor 2 on 60S subunits of 80S initiation complexes and polysomes. *Proc. Natl. Acad. Sci. USA.* 89:12063–12067.

Ramirez, M., R.C. Wek, C.R. Vazquez de Aldana, B.M. Jackson, B. Freeman, and A.G. Hinnebusch. 1992. Mutations activating the yeast eIF2α kinase GCN2: isolation of alleles altering the domain related to histidyl-tRNA synthetases. *Mol. Cell. Biol.* 12:5801–5815.

Sarkar, S., and A.K. Hopper. 1998. tRNA nuclear export in *Saccharomyces cerevisiae*: in situ hybridization analysis. *Mol. Biol. Cell.* 9:3041–3055.

Sheth, U., and R. Parker. 2003. Decapping and decay of messenger RNA occur in cytoplasmic processing bodies. *Science.* 300:805–808.

Sudhakar, A., A. Ramachandran, S. Ghosh, S.E. Hasnain, R.J. Kaufman, and K.V. Ramaiah. 2000. Phosphorylation of serine 51 in initiation factor 2α (eIF2α) promotes complex formation between eIF2α(P) and eIF2B and causes inhibition in the guanine nucleotide exchange activity of eIF2B. *Biochemistry.* 39:12929–12938.

Teixeira, D., U. Sheth, M.A. Valencia-Sanchez, M. Brengues, and R. Parker. 2005. Processing bodies require RNA for assembly and contain nontranslating mRNAs. *RNA.* 11:371–382.

van der Knaap, M., P. Leegwater, A. Konst, A. Visser, S. Naidu, C. Oudejans, R. Schutgens, and J. Pronk. 2002. Mutations in each of the five subunits of translation initiation factor eIF2B can cause leukoencephalopathy with vanishing white matter. *Ann. Neurol.* 51:264–270.

von der Haar, T., and J.E. McCarthy. 2002. Intracellular translation initiation factor levels in *Saccharomyces cerevisiae* and their role in cap-complex function. *Mol. Microbiol.* 46:531–544.

Wang, X., F.E. Paulin, L.E. Campbell, E. Gomez, K. O'Brien, N. Morrice, and C.G. Proud. 2001. Eukaryotic initiation factor 2B: identification of multiple phosphorylation sites in the epsilon-subunit and their functions in vivo. *EMBO J.* 20:4349–4359.

White, J., and E. Stelzer. 1999. Photobleaching GFP reveals protein dynamics inside live cells. *Trends Cell Biol.* 9:61–65.